Discovery of Singlet Diradicals: Theoretical Study on the Cage Species $C_{14}N_{12}-H_6$ and Its Six Derivatives

Hongwei Zhou,[†] Ning-Bew Wong,*[,†] Kai-Chung Lau,[†] Anmin Tian,[‡] and Wai-Kee Li[§]

Department of Biology and Chemistry, City University of Hong Kong, Kowloon, Hong Kong, Faculty of Chemistry, Sichuan University, Chengdu 610064, People's Republic of China, and Department of Chemistry, The Chinese University of Hong Kong, Shatin, Hong Kong

Received: March 29, 2007; In Final Form: July 25, 2007

In this work, the geometries, harmonic vibrational frequencies, and high-energy density material (HEDM) properties of a novel species and its six derivatives with the general formula $C_{14}N_{12}-R_6$ (R = H, OH, F, CN, N_3, NH_2, and NO_2) have been investigated at the restricted and unrestricted B3LYP/cc-pVDZ levels of theory. Natural bond orbital (NBO), natural orbital (NO), and atoms in molecules (AIM) analyses are applied to examine their electronic topologies. It is found that for the four species of R = H, CN, N_3, and NO_2, (1) there exist high LUMO occupation numbers, (2) there is considerable spin density congregated on the two central carbon atoms, (3) there exists through space interaction (or intramolecular interaction, which is one of the stabilizing factors of a diradicaloid) between the two central carbon atoms, (4) the distance (about 3 Å) between the two central carbon atoms (as the apexes of two trigonal pyramids with their bases facing each other) is suitable and favorable for diradical formation. All the results support that these four species are diradicals or diradicaloids. Furthermore, the appreciable singlet−triplet energy gaps indicate that these four diradicals tend to have a singlet ground state. There is a moderate HOMO−LUMO gap (on the order of 1.5 to 2.1 eV) for these four species. These four singlet diradicals may be novel organic semiconductor materials or nonlinear optical materials. On the other hand, the remaining three species, with R = OH, F, and NH_2, are not diradicaloids.

Introduction

Azabenzenes are categorized as an important parent molecular system for numerous compounds such as biologically active nicotinic acid and nucleotides cytosine, uracil, and thymine.[1,2] In particular, *s*-triazine-based species have various applications in the manufacturing of polymers, dyes, explosives, pesticides, and commodity chemicals.[3−7] Korkin and Bartlett[4] have suggested that the polymers of *s*-triazine, compared with their respective monomers, have increased densities and relative stabilities, as well as improved chemical properties. Among all the polymers, Pauling and Sturdivant[8] suggested tri-*s*-triazine ($C_6N_7H_3$, see Figure 1) rings as the common nucleus. In the past decades, $C_6N_7H_3$ was studied in detail, both experimentally[9−13] and theoretically.[14−17] Exchanging the nitrogen atoms with carbon atoms in tri-*s*-triazine (Figure 1) forms a new species $C_7N_6-H_6$ (Figure 2). Similar to the tri-*s*-triazine, it is an *s*-triazine-based molecule. It may be supposed that the chemical property of $C_7N_6-H_6$ is similar to that of tri-*s*-triazine. However, upon investigation by our group, it was found that planar $C_7N_6-H_6$ does not represent a local minimum on the potential energy surface (PES). This is possibly because of the unusual electronic structure at the central carbon atom (C6), on which there is an unpaired electron in its (non-bonded) hybrid orbital. When two $C_7N_6-H_6$ molecules are fused together by binding three carbon atoms in each frame in an alternative manner to form the cage species $C_{14}N_{12}-H_6$ (Figure 3), we have found that the "dimer"

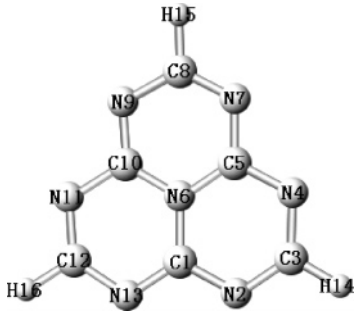

Figure 1. The geometrical structure of tri-*s*-triazine.

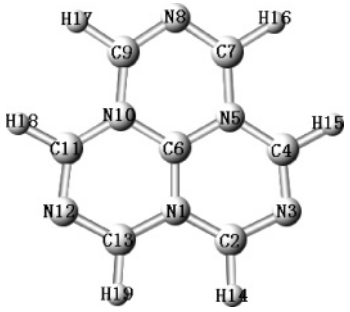

Figure 2. The geometrical structure of $C_7N_6-H_6$.

represents a minimum in the PES. This cage compound is the main object of this paper. Moreover, we have also studied its six derivatives with the general formula $C_{14}N_{12}-R_6$, where R = OH, F, CN, N_3, NH_2, and NO_2 (Figure 3). To our knowledge, there is no report on these systems up to now. The bonding

* Corresponding author: Ning-Bew Wong, E-mail: bhnbwong@cityu.edu.hk.
[†] City University of Hong Kong.
[‡] Sichuan University.
[§] The Chinese University of Hong Kong.

10.1021/jp072460l CCC: $37.00
Published on Web 09/11/2007

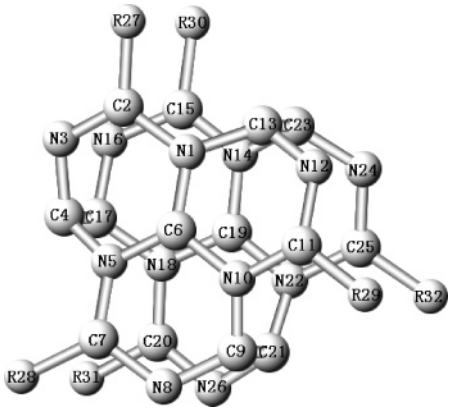

Figure 3. The geometrical structure of cage species $C_{14}N_{12}-R_6$, with R = H, OH, F, CN, N_3, NH_2, and NO_2.

properties, specifically the diradical character, of these species will be investigated in detail in this paper.

We will investigate the diradical properties of the seven cage species. A diradical has an even number of electrons, and two of these electrons are located at two separate atoms. Diradicals have been investigated extensively, both experimentally[18−28] and theoretically.[29−40] Detection of the diradicals in an experiment is difficult, possibly due to their high reactivities and short lifetimes.[18−22] Singlet diradicals are important intermediates in some organic reactions, such as ring opening of strained cycloalkanes.[20−22,29] Because of their potential applications in the field of molecular materials such as electrical conductors[28] and nanomaterials, singlet diradicals have drawn much interest and attention. Searching for the stable singlet diradicals remains a challenge to both experimental and theoretical scientists.

The stability of a diradical is affected by two factors. The first is the degree of interaction between the two radical sites. In general, the stronger the interaction, the more stable the diradical becomes, and the species has *less* diradical character. The diradical character vanishes when the interaction is strong enough to form a covalent bond. The second factor is the steric effects, including ring (or cage) strain, steric crowding, and substitution effects. The steric effects within the species may hinder the approaching of the two radical sites. A diradical with steric effects is predicted to be more stable than when there is no such effects.[39,40] The stability of the four diradicals found in this work is mainly due to steric effects.

On the whole, there are three characteristics for non-linear optical (NLO) materials: high stabilities, high first-, second-, and third-order polarizabilities, and low HOMO−LUMO energy gaps. Some studies[41,42] have suggested that the π-containing substituents such as azide and ethenyl result in a significant increase of first-, second-, and third-order polarizabilities and a significant decrease of the HOMO−LUMO gap. In semiconductor materials, there should be a moderate HOMO−LUMO gap[42] around 1.0−3.0 eV. In our system, the HOMO−LUMO gap of the species changes greatly with substituents. Some of the species studied may be potential novel organic semiconductor or NLO materials.

Methods

Density functional theory (DFT) has been applied to optimize the structures of the species and to predict the harmonic vibrational frequencies. Specifically, Becke's three-parameter hybrid functional with the Lee−Yang−Parr correlation functional (B3LYP) has been employed. Dunning's cc-pVDZ basis set has been used throughout, and the SCF convergence criterion is set to 10^{-8}. The single-point energy calculation has been also carried out at the MP2/cc-pVDZ level in order to identify the existence of the intramolecular interactions. All calculations were carried out using the GAUSSIAN98 program.[43] It is noted that the performance of UB3LYP calculations on diradicals has been investigated in comparison with the results obtained with other methods.[44,45] The comparison indicates that UB3LYP calculations are reliable in the qualitative analysis of a diradical. In any event, for relatively large species such as $C_{14}N_{12}-R_6$, it is impractical to perform high level *ab initio* calculations such as the coupled-cluster perfect-pairing (CC-PP) method proposed by Jung and Head−Gordon.[39] Indeed, the DFT method is a viable alternative.[44,45] The natural bond orbital (NBO)[46−49] analysis has been carried out at the B3LYP/cc-pVDZ level on the basis of the optimized geometries.

The topological properties of the charge density have been characterized using the atoms in molecules (AIM) theory of Bader[50] with the AIM 2000 program package.[51] The AIM approach provides a rigorous procedure based upon the topology of electronic density $\rho(r)$. It partitions the molecule into atomic fragments Ω bound by a zero flux surface for the gradient vector field of $\rho(r)$. A crucial element of the theory is the set of properties of the critical points in $\rho(r)$, where $-$r vanishes. The points lying between bonded atoms are called bond critical points (BCPs). Local properties at BCPs convey valuable information about the molecular electronic structure. It is noted that the results obtained from AIM analysis are not heavily dependent on the computational method,[52] because all the results benefit from being independent of the underlying computational scheme that yields the wave function.[53] More precisely, the wave functions can be Gaussian, Slater, or plane wave functions. They are stable with respect to basis set variation and exist within the framework of classic correlation methods, including DFT approaches. Hence we are justified to use the AIM results to verify the existence of the intramolecular interactions between the two supposed radical sites.

The main computational measure of a diradical character is the relative value of the occupation numbers for bonding and antibonding orbitals associated with the two radical sites.[39] The more closely the antibonding-orbital occupation number approaches 1.00, the closer the system is to a pure diradical and, correspondingly, the *less* stable of the diradical. Using this measurement, Jung and Head−Gordon[39] have explored some typical diradical or diradicaloid species quantitatively. This measure is applicable for diradicals in which the two radical sites tend to form a weak bond. In the case where the two radical sites do not tend to form a bond, and therefore there is no antibonding orbital between the two radical sites, we then consider through-space interaction (or intramolecular interaction) between the two supposed radical sites as well as spin densities on the radical sites to estimate the diradical character of a species.[40] Specifically, the distance between the unpaired electrons provides a direct assessment of the diradical character. Ma et al.[40] have identified some 1,3-diradicals qualitatively using this method. It is noted that, regardless of whether or not the two radical sites tend to form a bond, the HOMO and LUMO occupation numbers can be obtained from NO analysis. So, in this work, we use the molecular orbital occupation number instead of antibonding-orbital occupation number, the through-space (intramolecular) interaction, and spin densities of the two radical sites to measure the diradical character.

Predictions of the spin preference are usually confirmed by the complete active space self-consistent field (CASSCF) method, as implemented in the GAUSSIAN98 package. How-

TABLE 1: The Bond Lengths (Å) in the Frameworks of the Seven Cage Species $C_{14}N_{12}-R_6$

bond	H	OH	F	CN	N_3	NH_2	NO_2
N1−C2, N5−C7, N10−C11, N14−C15, N18−C20, N22−C25	1.408	1.389	1.389	1.421	1.404	1.400	1.404
N1−C6, N5−C6, C6−N10, N14−C19, N18−C19, C19−N22	1.386	1.451	1.451	1.363	1.390	1.451	1.378
N1−C13, C4−N5, C9−N10, N14−C23, C17−N18, C21−N22	1.453	1.454	1.453	1.475	1.458	1.456	1.459
C2−N3, C7−N8, C11−N12, C15−N16, C20−N26, N24−C25	1.296	1.297	1.280	1.306	1.302	1.306	1.284
N3−C4, N8−C9, N12−C13, N16−C17, C21−N26, C23−N24	1.420	1.411	1.412	1.392	1.415	1.409	1.419
C4−C17, C9−C21, C13−C23	1.357	1.368	1.368	1.400	1.354	1.367	1.352

TABLE 2: The Bonding Orbital Energies (au) in the Frameworks of the Seven Cage Species $C_{14}N_{12}-R_6$

bond	H	OH	F	CN	N_3	NH_2	NO_2
N1−C2, N5−C7, N10−C11	−0.83355	−0.84446	−0.89054	−0.89704	−0.85845	−0.80601	−0.92703
C6−N10, C19−N22	−0.84675	−0.77925	−0.82773	−0.94549	−0.85068	−0.74930	−0.93113
N1−C13, C4−N5, C9−N10	−0.78718	−0.75272	−0.80171	−0.84307	−0.79102	−0.72178	−0.85656
C2−N3, C7−N8, C11−N12	−0.88031	−0.87607	−0.93502	−0.93859	−0.90142	−0.82490	−0.98545
C2−N3, C7−N8, C11−N12[a]	−0.34961	−0.34358	−0.39137	−0.42114	−0.35733	−0.31926	−0.42782
N3−C4, N8−C9, N12−C13	−0.77253	−0.77110	−0.81439	−0.86600	−0.78296	−0.74200	−0.84417
C4−C17, C9−C21, C13−C23	−0.73608	−0.74096	−0.78367	−0.80552	−0.77031	−0.71464	−0.81391
C4−C17, C9−C21, C13−C23[a]	−0.38004	−0.34050	−0.38772	−0.40206	−0.36240	−0.31232	−0.44879
N1−C6	−0.84672	−0.77926	−0.82773	−0.94547	−0.85068	−0.74930	−0.93203
N1−C6[a]				−0.45670			
N5−C6	−0.84671	−0.77923	−0.82773	−0.94336	−0.85068	−0.74930	−0.93223
N5−C6[a]							−0.45895
N14−C19	−0.84672	−0.77926	−0.82773	−0.94547	−0.85068	−0.74930	−0.93203
N14−C19[a]				−0.45670			
N18−C19	−0.84671	−0.77923	−0.82773	−0.94336	−0.85068	−0.74930	−0.93223
N18−C19[a]							−0.45895
C6−C19[b]	−0.21599	−0.63214	−0.67774		−0.22485	−0.59706	

[a] NBO analysis shows that these are π−type orbitals. [b] NBO analysis shows that this is a σ orbital. It is regarded as a weak bond for R = OH, F, and NH_2. For R = H and N_3, judging from the orbital energy, the force between the two atoms may be considered as intramolecular interaction. There is no bonding orbital between C6 and C19 for R = CN and NO_2 in NBO analysis.

ever, it is quite expensive[40] to carry out the CASSCF optimizations for species such as $C_{14}N_{12}-R_6$. Therefore, the unrestricted DFT was employed to investigate their geometries, spin preferences, and singlet−triplet (S-T) gaps (ΔE_{S-T}) with the B3LYP functional and the cc-pVDZ basis set. The ΔE_{S-T} can be obtained by using the DFT ΔH_f difference introduced in our previous work.[54] It is pointed out that UB3LYP calculations generally yield ΔE_{S-T} values that are too small, when compared with their high-level *ab initio* counterparts.[40] The underestimation of ΔE_{S-T} by UB3LYP calculations has been ascribed to the mixing of wave functions for triplet state into the singlet state.[40] In other words, the "singlet" wave function obtained by unrestricted methods is not a pure singlet wave function. Instead, it is contaminated with the higher energy triplet wave functions, which can be reflected by the non-zero values of $\langle S^2 \rangle$. A proposed correction formula[55] may alleviate this problem to some extent by scaling off spin contaminations in the singlet. Since we are only interested in the qualitative trend in the singlet preference and are not concerned with the quantitative values of ΔE_{S-T}, only the uncorrected values are employed in our discussions.

Results and Discussion

The geometrical optimizations were successfully performed at the restricted and unrestricted B3LYP/cc-pVDZ levels. All of the vibrational frequencies of the species are positive (the lowest frequencies of the seven species at open-shell singlet state are listed in Table 1 in Supporting Information). The optimized bond lengths in the cage frameworks are listed in Table 1.

Bond Lengths. In Table 1, there are three C−C bonds and 30 C−N bonds. The lengths of the three C−C bond are shorter than that of a normal C−C single bond (about 1.47 Å) and longer than that of a normal C═C double bond (about 1.25 Å). So, we may conclude that they have some double bond character (also denoted as C═C from here on). The longest C═C bond length is 1.400 Å for R = CN, and the shortest one is 1.352 Å for R = NO_2. Among the 30 C−N bonds, the bond lengths of C2−N3, C7−N8, C11−N12, C15−N16, C20−N26, and C25−N24 range from 1.279 to 1.306 Å. Judging by the bond lengths, these six bonds should be considered as double bonds, as their lengths are very close to that of a normal C═N bond (about 1.27 Å). The remaining 24 C−N bonds are single bonds. The average lengths of these 24 C−N single bonds are 1.416, 1.426, 1.426, 1.412, 1.416, 1.429, and 1.415 Å for R = H, OH, F, CN, N_3, NH_2, and NO_2, respectively. As expected, the bond lengths of the cage frameworks vary with substituents, specifically, those around central atoms C6 and C19. This can be verified by the relatively large range (from 1.363 to 1.451 Å) of the bond lengths for C6−N1, C6−N5, C6−N10, C19−N14, C19−N18, and C19−N22 (see Table 1). On the other hand, the other C−N bond lengths, such as N1−C13 and C4−N5, fall in a very narrow range, from 1.453 to 1.475 Å. In the other words, the chemical properties of the cages are greatly influenced by the bonding characteristics at these two central atoms.

NBO Analysis. NBO analysis has been carried out for all seven cages based on structures optimized at the B3LYP/cc-pVDZ level. The orbital energies (OEs) of the seven cage frameworks are listed in Table 2. NBO analysis shows that there are 43 bonding orbitals for R = H, OH, F, N_3, and NH_2, and 44 bonding orbitals for R = CN and NO_2. The C6···C19 σ_{C-C} orbital exists in R = H, OH, F, N_3, and NH_2, but it does not exist in R = CN and NO_2 (see Table 2). The OEs of C6···C19 are −0.21599, −0.63214, −0.67774, −0.22485, and −0.59706 au for R = H, OH, F, N_3, and NH_2, respectively. The intramolecular interactions of C6···C19 for R = OH, F, and NH_2 are strong enough to be regarded as weak bonds, while the relatively high OE's for R = H and N_3 indicate that there is no bond formed between C6 and C19. NBO analysis shows

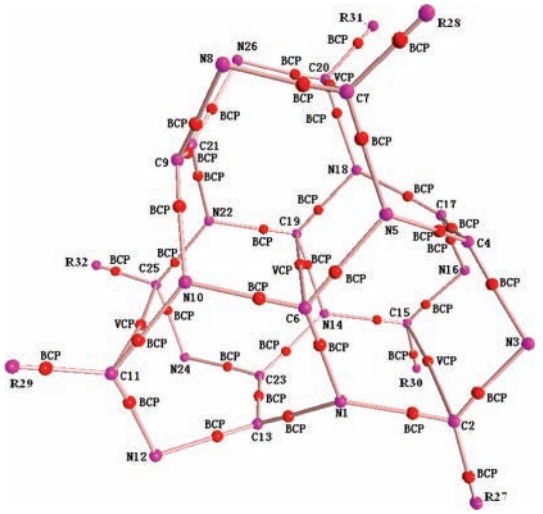

Figure 4. The bond critical points and the bond paths of cage species $C_{14}N_{12}-R_6$, with R = H, OH, F, CN, N_3, NH_2, and NO_2. BCP: bond critical point, VCP: intramolecular interaction, line: bond path.

that there are three σ_{C-C} orbitals and three π_{C-C} orbitals, that is, there are three C═C double bonds (C4═C17, C9═C21, and C13═C23) for each cage.From Table 2, it can be seen that both the σ_{C-C} OEs and π_{C-C} OEs vary with substituents. NBO analysis indicates that there are 30 σ_{C-N} orbitals and six π_{C-N} orbitals, that is, there are 24 C−N single bonds and six C═N double bonds in the molecules with R = H, OH, F, N_3 and NH_2. There are 30 σ_{C-N} orbitals and eight π_{C-N} orbitals, that is, there are 22 C−N single bonds and 8 C═N double bonds for R = CN and NO_2. As mentioned above, the chemical properties of the species are mainly dependent on the two central atoms C6 and C19, and the bonds formed by them (C6−N1, C6−N5, C6−N10, C19−N14, C19−N18, and C19−N22) in the cage framework. These OEs have a large range; clearly they vary with substituents.

AIM Analysis. The results of AIM analysis (Tables 3−9) show that negative $\nabla^2\rho$ values of BCP are associated with bond path (BP) lengths less than 1.6 Å. The threshold value of 1.6 Å is chosen since the length of a covalent bond is usually less than 1.6 Å at the B3LYP/cc-pVDZ level. In addition, the ellipticity (ϵ) values also reflect bond character. That is, a smaller ϵ value represents more σ-bond character and a larger ϵ value represents more π-bond character in the molecule. The bond strength is measured by the charge densities (ρ) between two atoms concerned. The results from AIM analysis also show that our seven cages have either one (R = OH, F, CN, N_3, NH_2) or four (R = H, NO_2) intramolecular interactions at the RB3LYP/cc-pVDZ and MP2/cc-pVDZ levels. It may be argued that the B3LYP functional does not address the intermolecular van der Waals interactions well because it does not include long-range correction (LC) in the generalized gradient approximation (GGA) exchange functional.[56,57] Hence, we carried out single-point energy calculations at the MP2/cc-pVDZ level in order to verify the existence of intramolecular interactions in these cages. Furthermore, Kosov and Popelier[52] have verified that the AIM results are not heavily method dependent, and DFT may also be used in this type of analysis, as we have found here. In Figure 4, the intramolecular interactions are denoted by VCP so as to distinguish them from the BCPs.

For R = H ($C_{14}N_{12}-H_6$), there are 33 BCPs with $\nabla^2\rho < 0$ and 4 BCPs with $\nabla^2\rho > 0$ in the $C_{14}N_{12}$ cage framework at the RB3LYP/cc-pVDZ level. So there are 33 covalent bonds and four intramolecular interactions (Figure 4). The intramolecular interactions are C6···C19, C2···C15, C7···C20, and C11···C25. The BP length of C6···C19 is 3.086 Å (see Table 3), which can be regarded as the approximate distance between atoms C6 and C19, as the BP is nearly a beeline. The ρ value of the BCP between C6 and C19 is only 0.010, indicating that the charge of the region is locally depleted. That is, there exists only a weak interaction between atoms C6 and C19. Furthermore, its $\nabla^2\rho$ value of 0.034 also indicates that the C6···C19 is not a covalent bond.

The BP length of C2···C15, C7···C20, and C11···C25 is 2.976 Å. Their ϵ values are 3.56, which is a large value indicating that these BPs have a considerable curvature. Their ρ values are 0.012, indicating that the charge of the region is also locally depleted, i.e., there is only intramolecular interaction between these atom pairs. Their $\nabla^2\rho$ value is 0.039, which indicates that C2···C15, C7···C20, and C11···C25 are not covalent bonds.

The BP length of C4−C17, C9−C21, and C13−C23, which connect frame-1 and frame-2 (the framework containing C_7N_6 atoms 1 to 13 is denoted as frame-1, while frame-2 contains atoms 14 to 26), is 1.358 Å (the bond lengths are 1.357 Å, see Table 1). Their ϵ value is 0.462; such a large value indicates that C4−C17, C9−C21, and C13−C23 bonds have some π character. Their ρ value is 0.330, indicating that the charge is locally concentrated in the regions between these atom pairs. Their $-\ ^2\rho$ value of −0.802 indicates that the three bonds connecting frame-1 and frame-2 are covalent bonds.

The BP lengths of C2−N3, C7−N8, C11−N12, C15−N16, C20−N26, and N24−C25 are 1.297 Å (the bond lengths are 1.296 Å, see Table 1). Their ϵ value is 0.313, indicating that these bonds have considerable π character. Their ρ value is 0.370, indicating that the charge is locally concentrated in the regions between these atom pairs. The $\nabla^2\rho$ value of −1.108 indicates that these six bonds are covalent bonds.

The BP length of N1−C2, N5−C7, N10−C11, N14−C15, N18−C20, and N22−C25 is 1.408 Å (the bond lengths are 1.408 Å, see Table 1). Their ϵ value of 0.113 indicates that these bonds are σ character. The ρ value of 0.283 indicates that the charge is locally concentrated in the regions between the atom pairs. The $\nabla^2\rho$ value of −0.779 indicates that these six bonds are covalent bonds. Upon examining Table 3, it is clear that the AIM results of the set of N1−C13, C4−N5, C9−N10, N14−C23, C17−N18, and C21−N22 are similar to this set.

The set of N1−C6, N5−C6, C6−N10, N14−C19, N18−C19, and C19−N22 are the bonds (equivalent by symmetry) formed by the two central atoms C6 in frame-1 and C19 in frame-2. Their ρ value is 0.308, which is greater than the corresponding values (0.283 and 0.259) of the previous two sets. It indicates that these six bonds are stronger than the bonds of the two previous sets.

Among the 37 BPs, the length of C6···C19 is the longest. It indicates that the two central atoms C6 and C19 are pointing outward from frame-1 and frame-2, respectively. That is, both frame-1 and frame-2 are convex, with C6 and C19 occupying their outermost points. It is noted that the AIM results of $C_{14}N_{12}-H_6$ and $C_{14}N_{12}-(NO_2)_6$ (Table 4) are very similar. Hence, no further discussion will be given for $C_{14}N_{12}-(NO_2)_6$. The AIM analysis results of $C_{14}N_{12}-(CN)_6$ (see Table 5) are similar to those of $C_{14}N_{12}-H_6$ except that the intramolecular interactions between C2 and C15, C7 and C20, and C11 and C25 do not exist in $C_{14}N_{12}-(CN)_6$. Furthermore, the AIM results of $C_{14}N_{12}-(N_3)_6$ (see Table 6) are essentially identical to those of $C_{14}N_{12}-(CN)_6$.

TABLE 3: The Bond Path Lengths (BPL, Å), the Ellipticities (ϵ), the Charge Densities (ρ), the Laplacian of ρ ($\nabla^2\rho$) of the Bonds or Intramolecular Interactions in the Cage Framework of $C_{14}N_{12}-H_6$

bond	BPL[a]	ϵ	ρ	$\nabla^2\rho$
N1−C2, N5−C7, N10−C11, N14−C15, N18−C20, N22−C25	1.408	0.113	0.283	−0.779
N1−C6, N5−C6, C6−N10, N14−C19, N18−C19, C19−N22	1.386	0.341	0.308	−0.920
N1−C13, C4−N5, C9−N10, N14−C23, C17−N18, C21−N22	1.453	0.123	0.259	−0.623
C2−N3, C7−N8, C11−N12, C15−N16, C20−N26, N24−C25	1.297	0.313	0.370	−1.108
N3−C4, N8−C9, N12−C13, N16−C17, C21−N26, C23−N24	1.420	0.093	0.297	−0.802
C4−C17, C9−C21, C13−C23	1.358	0.462	0.330	−0.802
C6−C19	3.086	0.004	0.010	0.034
C2−C15, C7−C20, C11−C25	2.976	3.569	0.012	0.039

[a] BPL is the sum of distance between the BCP and the first atom, and the distance between the BCP and the second atom.

TABLE 4: The Bond Path Lengths (BPL, Å), the Ellipticities (ϵ), the Charge Densities (ρ), the Laplacian of ρ ($\nabla^2\rho$) of the Bonds or Intramolecular Interactions in the Cage Framework of $C_{14}N_{12}-(NO_2)_6$

bond	BPL[a]	ϵ	ρ	$\nabla^2\rho$
N1−C2, N5−C7, N10−C11, N14−C15, N18−C20, N22−C25	1.403	0.161	0.290	−0.821
N1−C6, N5−C6, C6−N10, N14−C19, N18−C19, C19−N22	1.378	0.319	0.314	−0.961
N1−C13, C4−N5, C9−N10, N14−C23, C17−N18, C21−N22	1.459	0.119	0.255	−0.600
C2−N3, C7−N8, C11−N12, C15−N16, C20−N26, N24−C25	1.284	0.388	0.382	−1.093
N3−C4, N8−C9, N12−C13, N16−C17, C21−N26, C23−N24	1.419	0.108	0.296	−0.810
C4−C17, C9−C21, C13−C23	1.354	0.510	0.332	−0.807
C6−C19	3.024	0.003	0.011	0.037
C2−C15, C7−C20, C11−C25	3.028	7.864	0.011	0.039

[a] BPL is the sum of distance between the BCP and the first atom, and the distance between the BCP and the second atom.

TABLE 5: The Bond Path Lengths (BPL, Å), the Ellipticities (ϵ), the Charge Densities (ρ), the Laplacian of ρ ($\nabla^2\rho$) of the Bonds or Intramolecular Interactions in the Cage Framework of $C_{14}N_{12}-(CN)_6$

bond	BPL[a]	ϵ	ρ	$\nabla^2\rho$
N1−C2, N5−C7, N10−C11, N14−C15, N18−C20, N22−C25	1.421	0.174	0.278	−0.744
N1−C6, N5−C6, C6−N10, N14−C19, N18−C19, C19−N22	1.362	0.227	0.329	−1.069
N1−C13, C4−N5, C9−N10, N14−C23, C17−N18, C21−N22	1.474	0.111	0.245	−0.538
C2−N3, C7−N8, C11−N12, C15−N16, C20−N26, N24−C25	1.307	0.374	0.363	−1.176
N3−C4, N8−C9, N12−C13, N16−C17, C21−N26, C23−N24	1.392	0.185	0.312	−0.930
C4−C17, C9−C21, C13−C23	1.400	0.463	0.303	−0.687
C6−C19	3.024	0.000	0.009	0.039
C2−C15, C7−C20, C11−C25	–	–	–	–

[a] BPL is the sum of distance between the BCP and the first atom, and the distance between the BCP and the second atom.

TABLE 6: The Bond Path Lengths (BPL, Å), the Ellipticities (ϵ), the Charge Densities (ρ), the Laplacian of ρ ($\nabla^2\rho$) of the Bonds or Intramolecular Interactions in the Cage Framework of $C_{14}N_{12}-(N_3)_6$

bond	BPL[a]	ϵ	ρ	$\nabla^2\rho$
N1−C2, N5−C7, N10−C11, N14−C15, N18−C20, N22−C25	1.404	0.163	0.292	−0.854
N1−C6, N5−C6, C6−N10, N14−C19, N18−C19, C19−N22	1.389	0.334	0.305	−0.906
N1−C13, C4−N5, C9−N10, N14−C23, C17−N18, C21−N22	1.458	0.121	0.255	−0.603
C2−N3, C7−N8, C11−N12, C15−N16, C20−N26, N24−C25	1.302	0.324	0.372	−1.300
N3−C4, N8−C9, N12−C13, N16−C17, C21−N26, C23−N24	1.415	0.090	0.298	−0.816
C4−C17, C9−C21, C13−C23	1.356	0.484	0.332	−0.814
C6−C19	3.158	0.000	0.009	0.031
C2−C15, C7−C20, C11−C25	–	–	–	–

[a] BPL is the sum of distance between the BCP and the first atom, and the distance between the BCP and the second atom.

For R = OH, i.e., $C_{14}N_{12}-(OH)_6$, there are two noteworthy points when its AIM results (see Table 7) are examined. One is the absence of intramolecular interactions between pair of C2 and C15, C7 and C20, and C11 and C25. The other is concerned with the intramolecular interaction C6···C19. In this cage, the $\nabla^2\rho$ (−0.419) and ρ (0.217) values for C6···C19 indicate that the interaction between these two atoms is nearly a covalent bond. Moreover, the BP length is 1.642 Å which may be taken as an approximate distance between atoms C6 and C19. This value is larger than a normal C−C single bond length (about 1.47 Å) and smaller than a normal interaction distance (in the range of 1.8 to 3 Å). Contrary to $C_{14}N_{12}-H_6$, the two central atoms C6 and C19 in $C_{14}N_{12}-(OH)_6$ are pointing *inward* from frame-1 and frame-2, respectively. That is, both frame-1 and frame-2 are concave, and C6 and C19 are no longer occupying the outermost points of the two frames. Finally, it is noted that the AIM results of $C_{14}N_{12}-F_6$ (see Table 8) and $C_{14}N_{12}-(NH_2)_6$ (see Table 9) are almost very similar to those of $C_{14}N_{12}-(OH)_6$. Hence, there will be no additional discussion for these two cages.

According to the above discussion, the two central atoms C6 and C19 have special bonding patterns. There is no bond between these two atoms in the seven cages during structural optimization. Both C6 and C19 seem to be trivalent carbon atoms. Under this circumstance, the geometrical optimization was successfully performed at the restricted B3LYP/cc-pVDZ level. All vibrational frequencies of the species are positive, indicating that the structures are local minima and hence the species are stable or metastable. There must be some extra factors to stabilize the molecules with trivalent carbon atoms because the carbon atoms are commonly quadravalent in "normal" molecules. AIM analysis shows that there are intramolecular interactions in these molecules. Specifically, the

TABLE 7: The Bond Path Lengths (BPL, Å), the Ellipticities (ϵ), the Charge Densities (ρ), the Laplacian of ρ ($\nabla^2\rho$) of the Bonds or Intramolecular Interactions in the Cage Framework of $C_{14}N_{12}-(OH)_6$

bond	BPL[a]	ϵ	ρ	$\nabla^2\rho$
N1−C2, N5−C7, N10−C11, N14−C15, N18−C20, N22−C25	1.389	0.166	0.304	−0.931
N1−C6, N5−C6, C6−N10, N14−C19, N18−C19, C19−N22	1.452	0.117	0.278	−0.722
N1−C13, C4−N5, C9−N10, N14−C23, C17−N18, C21−N22	1.455	0.088	0.259	−0.612
C2−N3, C7−N8, C11−N12, C15−N16, C20−N26, N24−C25	1.298	0.305	0.376	−1.340
N3−C4, N8−C9, N12−C13, N16−C17, C21−N26, C23−N24	1.412	0.106	0.300	−0.831
C4−C17, C9−C21, C13−C23	1.368	0.461	0.328	−0.795
C6−C19	1.642	0.000	0.217	−0.419
C2−C15, C7−C20, C11−C25	–	–	–	–

[a] BPL is the sum of distance between the BCP and the first atom, and the distance between the BCP and the second atom.

TABLE 8: The Bond Path Lengths (BPL, Å), the Ellipticities (ϵ), the Charge Densities (ρ), the Laplacian of ρ ($\nabla^2\rho$) of the Bonds or Intramolecular Interactions in the Cage Framework of $C_{14}N_{12}-F_6$

bond	BPL[a]	ϵ	ρ	$\nabla^2\rho$
N1−C2, N5−C7, N10−C11, N14−C15, N18−C20, N22−C25	1.389	0.198	0.305	−0.922
N1−C6, N5−C6, C6−N10, N14−C19, N18−C19, C19−N22	1.451	0.116	0.278	−0.722
N1−C13, C4−N5, C9−N10, N14−C23, C17−N18, C21−N22	1.453	0.091	0.260	−0.614
C2−N3, C7−N8, C11−N12, C15−N16, C20−N26, N24−C25	1.280	0.392	0.388	−1.307
N3−C4, N8−C9, N12−C13, N16−C17, C21−N26, C23−N24	1.412	0.111	0.299	−0.833
C4−C17, C9−C21, C13−C23	1.368	0.464	0.327	−0.792
C6−C19	1.646	0.000	0.216	−0.414
C2−C15, C7−C20, C11−C25	–	–	–	–

[a] BPL is the sum of distance between the BCP and the first atom, and the distance between the BCP and the second atom.

TABLE 9: The Bond Path Lengths (BPL, in Å), the Ellipticities (ϵ), the Charge Densities (ρ), the Laplacian of ρ ($\nabla^2\rho$) of the Bonds or Intramolecular Interactions in the Cage Framework of $C_{14}N_{12}-(NH_2)_6$

bond	BPL[a]	ϵ	ρ	$\nabla^2\rho$
N1−C2, N5−C7, N10−C11, N14−C15, N18−C20, N22−C25	1.400	0.141	0.295	−0.868
N1−C6, N5−C6, C6−N10, N14−C19, N18−C19, C19−N22	1.452	0.116	0.277	−0.721
N1−C13, C4−N5, C9−N10, N14−C23, C17−N18, C21−N22	1.456	0.086	0.258	−0.604
C2−N3, C7−N8, C11−N12, C15−N16, C20−N26, N24−C25	1.307	0.279	0.368	−1.290
N3−C4, N8−C9, N12−C13, N16−C17, C21−N26, C23−N24	1.409	0.097	0.302	−0.842
C4−C17, C9−C21, C13−C23	1.368	0.450	0.328	−0.796
C6−C19	1.652	0.000	0.213	−0.406
C2−C15, C7−C20, C11−C25	–	–	–	–

[a] BPL is the sum of distance between the BCP and the first atom, and the distance between the BCP and the second atom.

intramolecular interaction between atoms C6 and C19 is so strong for R = OH, F and NH_2 that a bond is formed between these two atoms. As a result, the two central atoms turn "inward" and frame-1 and frame-2 become concave. Thus, atoms C6 and C19 of these three species are quadravalent, if we take the weak bond between these two atoms as normal covalent bonds. On the other hand, for the remaining four species, atoms C6 and C19 do not follow the general valence, as the intramolecular interaction between them is too weak to be regarded as a covalent bond. As will be shown in the following discussion, there is a single electron on each of these two atoms in these four species. Hence they may be regarded as diradicals.

Singlet Diradical Characteristics. The unrestricted density functional theory (DFT) was employed to investigate the geometries, spin preferences, and S-T gaps (ΔE_{S-T}) of the seven species with the B3LYP functional and cc-pVDZ basis set. The results show that, for R = OH, F, and NH_2, both RB3LYP and UB3LYP formalisms yield similar shapes for the singlet state. For the triplet state using UB3LYP formalism, we failed to obtain SCF convergence. So the spin density (Table 10) and the isotropic Fermi contact couplings (FCCs, Table 2 in Supporting Information) at C6 and C19 are 0.0, and there is no net spin density for these three species as well. As mentioned above, the two central atoms C6 and C19 in these three cages turn inward to form a weak covalent bond. Hence, they are not diradicals. In order lend support to these conclusions, we have carried out additional calculations with different basis sets and at different levels of theory, including UHF/6-31G(d), UHF/6-31G, UHF/cc-pVDZ, UB3LYP/6-31G, UHFB/6-31G, and UHFS/6-31G for all seven species at open-shell singlet state, and CASSCF(4,6)/6-31G and GVB(3)/6-31G for R = H. Among these eight sets of additional calculations, UHF/6-31G(d) calculations did not achieve SCF convergence. For the UHFB/6-31G and UHFS/6-31G calculations, only restricted results were obtained, i.e., $\langle S^2\rangle = 0$. These results suggest that pure DFT may not be appropriate for diradicals or diradicaloids. Meanwhile, CASSCF(4,6)/6-31G and GVB(3)/6-31G calculations[61] were terminated because of insufficient computer resource. The results of the UHF/6-31G, UHF/cc-pVDZ, and UB3LYP/6-31G calculations are listed in Tables 3 and 4 of Supporting Information. It is found that, straight Hartree−Fock methods are also inappropriate for diradicals or diradicaloids, even though some of our species did achieve SCF convergence. For the UHF/cc-pVDZ calculations with open-shell singlet state, the results of R = H, OH, and NH_2 indicate that these species resemble multiple radicals as they possess many (more than two) radical sites. On the other hand, unrestricted B3LYP/6-31G calculations with singlet state for all seven species were completed successfully, and the results agree with those of unrestricted B3LYP/cc-pVDZ. Hence, we may state that the additional calculations we carried out support the main conclusions of this paper.

For R = H, there is no change in the molecular shape (now C6 and C19 occupy the outermost points of the two frames) whether the calculations are carried out by using RB3LYP or UB3LYP (at either the singlet or the triplet state), but the total

TABLE 10: The $\langle S^2 \rangle$ Values, the Spin Densities of the Central Atoms C6 and C19, the Absolute Spin Density Sum of All Atoms (Total) of the Seven Species at Singlet and Triplet States at the UB3LYP/cc-pVDZ Level

	singlet				triplet[b]			
R	$\langle S^2 \rangle$	C6	C19	Total	$\langle S^2 \rangle$	C6	C19	Total
H	0.79	0.54	−0.54	1.68	2.01	0.63	0.63	2.00
OH	0	0	0	0	–	–	–	–
F	0	0	0	0	–	–	–	–
CN	0.76	0.49	−0.49	1.72	2.02	0.59	0.59	2.00
N_3	0.87	0.59	−0.59	1.82	2.01	0.65	0.65	2.03
NH_2	0	0	0	0	–	–	–	–
NO_2	0.74	0.48	0.48	1.72	2.01	0.61	0.61	2.09
I[a]	1.01	0.99	−0.99	2.40	2.09	0.99	0.99	2.65
II[a]	1.01	1.00	−1.00	2.08	2.01	1.01	1.01	2.68

[a] These are the two reference diradicals shown in Scheme 1. The two diradical sites are atoms C1 and C4 for **I**, and C1 and C3 for **II**. It is noted that the corresponding numbers are all zero for a normal molecule such as ethane. [b] For R = OH, F, and NH_2, SCF convergence not achieved for the triplet state.

TABLE 11: The Total Energies (in au, Including Zero Point Corrections), the DFT ΔH_f (kcal mol^{-1}) of the Seven Species $C_{14}N_{12}-R_6$ at RB3LYP/cc-pVDZ and UB3LYP/cc-pVDZ (Singlet State and Triplet State)

	E_0 (au)			ΔH_f			
R	RB3LYP	singlet	triplet[b]	RB3LYP	singlet	triplet[b]	ΔE_{S-T}
H	−1193.55011	−1193.55462	−1193.54827	469.0	465.9	469.9	−4.0
OH	−1645.02996	−1645.02997	–	121.8	121.8	–	–
F	−1789.12263	−1789.12264	–	131.8	131.8	–	–
CN	−1746.94160	−1746.97802	−1746.97153	732.1	709.0	713.1	−3.1
N_3	−2175.19135	−2175.19892	−2175.19416	865.0	860.0	862.9	−2.9
NH_2	−1525.75320	−1525.75318	–	385.3	385.3	–	–
NO_2	−2420.55355	−2420.55581	−2420.51646	439.6	438.3	442.2	−3.8
I[a]		−195.12771	−195.12887		68.1	67.3	0.8
II[a]		−155.80204	−155.80465		97.7	96.1	1.6

[a] The ΔH_f of the two reference diradicals. [b] For R = OH, F, and NH_2, SCF convergence was not achieved for the triplet state.

TABLE 12: The Occupation Numbers (Singlet State) of the HOMO and LUMO Obtained from NO Analysis at the Level of UB3LYP/cc-pVDZ and the Occupation Numbers of the LUMO Obtained from NBO Analysis at the Levels of RB3LYP/cc-pVDZ and UB3LYP/cc-pVDZ (Singlet and Triplet)

	NO[a]		NBO[d]		
R	HOMO[b]	LUMO[c]	RB3LYP[e]	singlet[f]	triplet[g]
H	1.476	0.524	0.739	0.749	0.102
OH	2.000	0.000	0.334	0.334	0.334
F	2.000	0.000	0.282	0.282	0.282
CN	1.506	0.494	0.676	0.869	0.101
N_3	1.378	0.622	0.733	0.736	0.181
NH_2	2.000	0.000	0.348	0.348	0.348
NO_2	1.526	0.474	0.605	0.600	0.313
I[h]	1.014	0.986	0.239	0.074[i]	0.075[i]
II[h]	1.027	0.973	0.271	0.059[j]	0.061[j]

[a] The results obtained from natural orbital (NO) analysis. [b] The occupation numbers of HOMO at the level of UB3LYP/cc-pVDZ. [c] The occupation numbers of LUMO at the level of UB3LYP/cc-pVDZ. [d] The results obtained from natural bonding orbital (NBO) analysis. [e] The occupation numbers of LUMO at the level of RB3LYP/cc-pVDZ. [f] The occupation numbers of LUMO at the level of UB3LYP/cc-pVDZ (singlet). [g] The occupation numbers of LUMO at the level of UB3LYP/cc-pVDZ (triplet). [h] The two reference diradicals shown in Scheme 1. [i] There is no bond between C1 and C4 at the level of UB3LYP/cc-pVDZ. However, one lone electron is found on each atom. The values 0.074 and 0.075 are occupation number of the antibonding lone pair orbitals. [j] There is no bond between C1 and C3 at the level of UB3LYP/cc-pVDZ. However, one lone electron is found on each atom. The values 0.059 and 0.061 are occupation number of the antibonding lone pair orbitals.

energies (including zero-point energy corrections, see Table 11), spin contaminations, atomic spin densities at C6 and C19, and sum of absolute atomic spin densities are different. The total energies are −1193.550110, −1193.554622, and −1193.548274 au for RB3LYP, unrestricted singlet state and triplet state, respectively. The corresponding ΔH_fs are 469.0, 465.9, and 469.9 kcal mol^{-1}. At the unrestricted singlet state, the spin contamination $\langle S^2 \rangle = 0.79$ (see Table 10) and the atomic spin density at C6 and C19 is 0.54 (α electron) and −0.54 (β electron), respectively, and the sum of absolute atomic spin densities is 1.68 (the spin densities of the remaining atoms are too low to be listed). At the triplet state, the spin contamination $\langle S^2 \rangle = 2.01$, the atomic spin density at both C6 and C19 is 0.63 (α electron), and the sum of absolute atomic spin densities is 2.00. It can be seen that the unpaired electrons at C6 and C19 have opposite spin in the unrestricted singlet state, and the spins become parallel at the triplet state. The S-T gap (ΔE_{S-T}) of the species is −4.0 kcal mol-1, with singlet being the ground state. The diradical feature in cages with R = CN, N_3, and NO_2 are very similar to that found in $C_{14}N_{12}-H_6$ (see Tables 10 and 11).

By using the orbital phase theory, Ma et al.[40] studied the carbon-centered 1,3-diradicals qualitatively and concluded that through-space interactions (i.e., intramolecular interactions) result in the stability of the locally excited electronic configurations (i.e., diradicals) of the species. In this model of diradicals, a triplet diradical has two electrons of the same spin occupying two separate orbitals, whereas a singlet diradical is defined as

SCHEME 1: The Two Reference Diradicals from Ref 39

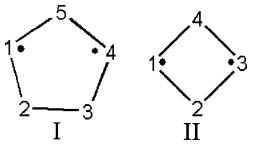

two electrons with opposite spins occupying two different orbitals. The diradical character of the species cannot be measured quantitatively in this model. As mentioned in Methods, the main computational measure of a diradical character is the relative value of the occupation numbers for bonding and antibonding orbitals associated with the two radical sites.[39] The balanced bonding and antibonding occupation numbers can be obtained from the perfect-pairing (PP) method, and the coupled-cluster (CC) formulation[58,59] of PP has been developed in the Q-Chem program.[60] Since our species are too large for such a treatment, we have selected to employ the UB3LYP/cc-pVDZ calculation instead. Based on the optimized structures, NBO analysis is carried out to obtain the occupation numbers. However, the bonding and antibonding occupation numbers obtained from NBO analysis are either exactly 0 or exactly 2 when the HOMO and LUMO are mixed to destroy $\alpha-\beta$ and spatial symmetries. Thus the two radical sites do not form a bond. So, NBO analysis partitions the whole two electrons to HOMO (giving rise to occupation number of 2) and partitions no electron to LUMO (with occupation number being 0). Jung and Head−Gordon[39] were aware of this deficiency of the NBO occupation numbers and hence suggested that DFT should not be inappropriate for diradicals. So, in this work, to obtain the rational occupation numbers, we employ NBO analysis at the RB3LYP/cc-pVDZ level without HOMO−LUMO mixing and NO analysis at the UB3LYP/cc-pVDZ level with HOMO−LUMO mixing. The results are listed in Table 12. Though these two methods do not yield the same numerical results, both sets of occupation numbers do predict diradical character of the species.

To verify that the reliability of NO occupation number obtained at the UB3LYP/cc-pVDZ level in estimating the diradical character, we carried out calculations of two known diradicaloid species,[39] shown in Scheme 1, at the UB3LYP/cc-pVDZ level. Subsequently, NBO and NO analyses were performed. The results are included in Tables 10−13. The diradical sites of the two reference species possess the highest spin densities both at the singlet state (0.99 for atoms C1 and C4 of species **I** and 1.00 for atoms C1 and C3 of species **II**, Table 10) and at the triplet state (0.99 for atoms C1 and C4 of species **I** and 1.01 for atoms C1 and C3 of species **II**). The LUMO occupation numbers obtained from NO analysis are 0.986 for species **I** and 0.973 for species **II**. That is, using NO analysis based on the UB3LYP calculation, the two reference species **I** and **II** can also be identified as diradicals qualitatively. The positive ΔE_{S-T} values (1.6 kcal mol^{-1} for **I** and 0.8 kcal mol^{-1} for **II**) indicate that the triplet state is more stable than the singlet state for both **I** and **II** because the ring closure reaction occurs easily for singlet 1,3-diradicals.[39,40] These results indicate that the HOMO−LUMO occupation number obtained from UB3LYP calculation can serve as a qualitative indicator for diradical character.

On the other hand, the HOMO−LUMO occupation numbers for species **I** and **II** using NBO analysis are inadequate to be qualitative indicators for diradical character. For **I**, there is no bond between C1 and C4 at the UB3LYP/cc-pVDZ level. However, nearly a half lone pair (not one electron) is found on each atom with occupation numbers for lone pair orbital (denoted by LP in NBO analysis) 0.934 for singlet and 0.933 for triplet. The values 0.074 and 0.075 in Table 12 are occupation numbers of the antibonding lone pair orbitals (denoted by LP* in NBO analysis). Similarly, for **II**, the occupation numbers of LP orbital are 0.936 for singlet and 0.938 for triplet, while those of LP* are 0.059 and 0.061. That is, we can only find part of a lone pair on each radical site; whether or not the lone pair represents an unpaired electron (as it is necessary for a diradical) is not entirely certain in NBO analysis. From Table 12, one can also find that the LUMO occupation numbers are significantly different in the NO and NBO results. In the former, the LUMO is nearly half filled; in the latter, there is hardly any occupation. Clearly, the NO analysis results are favorable for estimating the diradical character of the species studied.

It is found that the occupation numbers of HOMOs of the four supposed singlet diradicals are 1.476, 1.506, 1.378, and 1.526 for R = H, CN, N_3, NO_2, respectively. The corresponding occupation numbers of LUMOs are 0.524, 0.494, 0.622, and 0.474, respectively. These results indicate that there is a certain amount of electron excitation in each species. The LUMO occupation numbers of the four species are much less than 1.0, indicating that they are diradicaloids instead of pure diradicals.[39] As noted previously, low LUMO occupation decreases the diradical character but increases the stabilities of the species.[39] So, the four species are fairly stable diradicaloids. Finally, it is further pointed out that these diradicals represent local minima on the potential energy surfaces, and hence they are not transition states. The diradical stability of these four species is mainly due to the steric effects such as ring and/or cage strain. It is expected that the singlet diradical properties will impact a wide application as intermediates for the synthesis of nanomaterials.

The Characteristics of Organic Semiconductor Materials. In organic semiconductor materials, their HOMO−LUMO gaps

TABLE 13: The HOMO (au), LUMO (au), and Their Gap (eV) of the Seven Species at the Level RB3LYP/cc-pVDZ and at Singlet and Triplet States at the Level of UB3LYP/cc-pVDZ

	RB3LYP			singlet			triplet		
R	HOMO	LUMO	GAP	HOMO	LUMO	GAP	HOMO	LUMO	GAP
H	−0.15581	−0.08881	1.8232	−0.16082	−0.10099	1.6281	−0.16342	−0.09547	1.8490
OH	−0.23062	−0.05486	4.7827	−0.23062	−0.05486	4.7827	−0.23063	−0.05484	4.7835
F	−0.27375	−0.10019	4.7228	−0.27377	−0.10029	4.7207	−0.27377	−0.10029	4.7207
CN	−0.19804	−0.17580	0.6052	−0.22639	−0.17126	1.5002	−0.22655	−0.16684	1.6248
N_3	−0.16243	−0.10392	1.5922	−0.16955	−0.11624	1.4507	−0.17682	−0.10597	1.9279
NH_2	−0.20113	−0.03016	4.6524	−0.20116	−0.03020	4.6521	−0.20112	−0.03015	4.6524
NO_2	−0.23188	−0.17534	1.5385	−0.24624	−0.17065	2.0569	−0.23594	−0.17711	1.6009
I[a]				−0.18114	−0.03645	3.9372	−0.17931	−0.04000	3.7908
II[a]				−0.19170	−0.04401	4.0189	−0.18698	−0.04943	3.7430

[a] The two reference diradicals shown in Scheme 1.

should range from 1.0 to 3.0 eV.[42] The HOMOs, LUMOs, and their gaps at RB3LYP/cc-pVDZ, and at singlet and triplet states of UB3LYP/cc-pVDZ, are listed in Table 13. It can be seen in Table 13 that, for the four singlet diradicals, the HOMO−LUMO gaps are from 1.5 to 2.1 eV, while, for the three remaining cages, the HOMO−LUMO gaps are about 4.7 eV. It may thus be concluded that our four singlet diradicals are potential organic semiconductor materials. Furthermore, upon examining Table 11, all seven species are highly energetic thermodynamically, indicating that they may be potential HEDMs.

Conclusion

The NBO, NO, and AIM analyses have been used to examine the electronic topologies of cage species $C_{14}N_{12}-H_6$ and its six derivatives. The steric effects, ΔE_{S-T} values, spin density, spin contamination, and LUMO occupation numbers obtained from NO and NBO are used to explain the diradical character. Some predictions on the seven species have been drawn from the above discussions: (1) The seven species can be divided into two sets. One set consists of three normal molecules with R = OH, F, and NH_2. The other set is composed of four diradicaloids with R = H, CN, N_3, and NO_2. In these diradicaloids, C6 and C19 are the two radical sites. (2) The molecular structures in the two sets are quite different from each other. For the three normal molecules, atoms C6 and C19 are concave inward, while for the four diradicaloids, these two atoms are convex outward. (3) The LUMO occupation numbers, spin populations, atomic spin densities, and the isotropic Fermi contact couplings at UB3LYP/cc-pVDZ show that the three species in the first set are normal molecules, and the four species in second set are diradicals or diradicaloids with singlet ground state. (4) The four singlet diradicals have moderate HOMO−LUMO energy gaps (1.5−2.1 eV), and hence the species may be excellent organic semiconductor or NLO materials.

Acknowledgment. This work was supported by the Strategic Grant from City University of Hong Kong (Account No. 7001974) and the National Science Foundation of China (No. 20373045).

Supporting Information Available: The Cartesian coordinates of the species $C_{14}N_{12}-H_6$ and its six derivatives $C_{14}N_{12}-R_6$ at singlet states, Fermi contact couplings, $\langle S^2 \rangle$ values, spin densities, and occupation numbers. This material is available free of charge via the Internet at http://pubs.acs.org.

References and Notes

(1) Fulscher, M. P.; Andersson, K.; Roos, B. O. *J. Phys. Chem.* **1992**, *96*, 9204.
(2) Innes, K. K.; Roos, I. G.; Moomaw, W. R. *J. Mol. Spectrosc.* **1988**, *132*, 492.
(3) Zhan, Z.; Müllner, M.; Lercher, J. A. *Catal. Today* **1996**, *27*, 167.
(4) Korkin, A. A.; Bartlett, R. J. *J. Am. Chem. Soc.* **1996**, *118*, 12244.
(5) Wilson, E. K. *Chem. Eng. News* **2000**, *78*, 62.
(6) Liebig, J. *Ann. Pharm.* **1834**, *10*, 10.
(7) Gmelin, L. *Ann. Pharm.* **1835**, *15*, 252.
(8) Pauling, L.; Sturdivant, J. H. *Proc. Natl. Acad. Sci. U.S.A.* **1937**, *23*, 615.
(9) Rossman, M. A.; Leonard, N. J.; Urano, S.; LeBreton, P. R. *J. Am. Chem. Soc.* **1985**, *107*, 3884.
(10) Hosmane, R. S.; Rossman, M. A.; Leonard, N. J. *J. Am. Chem. Soc.* **1982**, *104*, 5497.
(11) Shahbaz, M.; Urano, S.; LeBreton, P. R.; Rossman, M. A.; Hosmane, R. S.; Leonard, N. J. *J. Am. Chem. Soc.* **1984**, *106*, 2805.
(12) Rossman, M. A.; Hosmane, R. S.; Leonard, N. J. *J. Phys. Chem.* **1984**, *88*, 4324.
(13) Kroke, E.; Schwarz, M.; Bordon, E. H.; Kroll, P.; Noll, B.; Norman, A. D. *New J. Chem.* **2002**, *26*, 508.
(14) Zheng, W. X.; Wong, N.-B.; Wang, W. Z.; Zhou, G.; Tian, A. M. *J. Phys. Chem. A* **2004**, *108*, 97.
(15) Zheng, W. X.; Wong, N.-B.; Zhou, G.; Liang, X. Q.; Li, J. S.; Tian, A. M. *New J. Chem.* **2004**, *28*, 275.
(16) Zheng, W. X.; Wong, N.-B.; Liang, X. Q.; Long, X. P.; Tian, A. M. *J. Phys. Chem. A* **2004**, *108*, 840.
(17) Zheng, W. X.; Wong, N.-B.; Li, W.-K.; Tian, A. M. *J. Phys. Chem. A* **2004**, *108*, 11721.
(18) Berson, J. A. *Science* **1994**, *266*, 1338.
(19) Pedersen, S.; Herek, J. L.; Zewail, A. H. *Science* **1994**, *266*, 1359.
(20) Buchwalter, S. L.; Closs, G. L. *J. Am. Chem. Soc.* **1975**, *97*, 3857.
(21) Jain, R.; Sponsler, M. B.; Coms, F. D.; Dougherty, D. A. *J. Am. Chem. Soc.* **1988**, *110*, 1356.
(22) Zewail, A. H. *Angew. Chem., Int. Ed.* **2000**, *39*, 2586.
(23) Adam, W.; Harrer, H. M.; Kita, F. W.; Nau, M. *Pure Appl. Chem.* **1997**, *69*, 91.
(24) Abe, M.; Adam, W. *J. Chem. Soc., Perkin Trans. 2* **1998**, 1063.
(25) Adam, W.; Borden, W. T.; Burda, C.; Foster, H.; Heidenfelder, T.; Heubes, M. D.; Hrovat, A.; Kita, F.; Lewis, S. B.; Scheutzow, D.; Wirz, J. *J. Am. Chem. Soc.* **1998**, *120*, 593.
(26) Abe, M.; Adam, W.; Heidenfelder, T. W.; Nau, M.; Zhang, X. *J. Am. Chem. Soc.* **2000**, *122*, 2019.
(27) Adam, W.; Baumgarten, M.; Maas, W. *J. Am. Chem. Soc.* **2000**, *122*, 6735.
(28) Wentrup, C. *Science* **2002**, *295*, 1846.
(29) Scheschewitz, D.; Amii, H.; Gornitzka, H.; Schoeller, W. W.; Bourissou, D.; Bertrand, G. *Science* **2002**, *295*, 1880.
(30) Grützmacher, H.; Breher, F. *Angew. Chem., Int. Ed.* **2002**, *41*, 4006.
(31) Hoffmann, R. *J. Am. Chem. Soc.* **1968**, *90*, 1475.
(32) Hoffmann, R.; Swaminathan, S.; Odell, B. G.; Gleiter, R. *J. Am. Chem. Soc.* **1970**, *92*, 7091.
(33) Getty, S. J.; Davidson, E. R.; Borden, W. T. *J. Am. Chem. Soc.* **1992**, *114*, 2085.
(34) Getty, S. J.; Hrovat, D. A.; Xu, J. D.; Barker, S. A.; Borden, W. T. *J. Chem. Soc., Faraday Trans.* **1994**, *90*, 1689.
(35) Baldwin, J. E.; Yamaguchi, Y.; Schaefer, H. F., III. *J. Phys. Chem.* **1994**, *98*, 7513.
(36) Schmidt, O.; Fuchs, A.; Gudat, D.; Nieger, M.; Hoffbauer, W.; Niecke, E.; Schoeller, W. W. *Angew. Chem., Int. Ed.* **1998**, *37*, 949.
(37) Skancke, A.; Hrovat, D. A.; Borden, W. T. *J. Am. Chem. Soc.* **1998**, *120*, 7079.
(38) Iwamoto, T.; Yin, D.; Kabuto, C.; Kira, M. *J. Am. Chem. Soc.* **2001**, *123*, 12730.
(39) Jung, Y.; Head-Gordon, M. *ChemPhysChem* **2003**, *4*, 522.
(40) Ma, L.; Ding, Y. H.; Hattori, K.; Inagaki, S. *J. Org. Chem.* **2006**, *69*, 4245.
(41) Zheng, W. X.; Wong, N.-B.; Li, W.-K.; Tian, A. M. *J. Chem. Theor. Comput.* **2006**, *2*, 808.
(42) Sun, M. T. *Chem. Phys.* **2006**, *320*, 155.
(43) Frisch, M. J.; Trucks, G. W.; Schlegel, H. B.; Scuseria, G. E.; Robb, M. A.; Cheeseman, J. R.; Zakrzewski, V. G.; Montgomery, J. A., Jr.; Stratmann, R. E.; Burant, J. C.; Dapprich, S.; Millam, J. M.; Daniels, A. D.; Kudin, K. N.; Strain, M. C.; Farkas, O.; Tomasi, J.; Barone, V.; Cossi, M.; Cammi, R.; Mennucci, B.; Pomelli, C.; Adamo, C.; Clifford, S.; Ochterski, J.; Petersson, G. A.; Ayala, P. Y.; Cui, Q.; Morokuma, K.; Malick, D. K.; Rabuck, A. D.; Raghavachari, K.; Foresman, J. B.; Cioslowski, J.; Ortiz, J. V.; Stefanov, B. B.; Liu, G.; Liashenko, A.; Piskorz, P.; Komaromi, I.; Gomperts, R.; Martin, R. L.; Fox, D. J.; Keith, T.; Al-Laham, M. A.; Peng, C. Y.; Nanayakkara, A.; Gonzalez, C.; Challacombe, M.; Gill, P. M. W.; Johnson, B. G.; Chen, W.; Wong, M. W.; Andres, J. L.; Head−Gordon, M.; Replogle, E. S.; Pople, J. A. *Gaussian 98*, revision A.11; Gaussian, Inc.: Pittsburgh, PA, 1998.
(44) (a) Zhang, D. Y.; Hrovat, D. A.; Abe, M.; Borden, W. T. *J. Am. Chem. Soc.* **2003**, *125*, 12823. (b) Abe, M.; Adam, W.; Borden, W. T.; Hattori, M.; Hrovat, D. A.; Nojima, M.; Nozaki, K.; Wirz, J. *J. Am. Chem. Soc.* **2004**, *126*, 574. (c) Brown, E. C.; Borden, W. T. *J. Phys. Chem. A* **2002**, *106*, 2963.
(45) Cremer, D.; Filatov, M.; Polo, V.; Kraka, E.; Shaik, S. *Int. J. Mol. Sci.* **2002**, *3*, 604.
(46) Carpenter, J. E.; Weinhold, F. *J. Mol. Struct. (THEOCHEM)* **1988**, *169*, 41.
(47) Reed, A. E.; Curtiss, L. A.; Weinhold, F. *Chem. Rev.* **1988**, *88*, 899.
(48) Foster, J. P.; Weinhold, F. *J. Am. Chem. Soc.* **1980**, *102*, 7211.
(49) Reed, A. E.; Weinstock, R. B.; Weinhold, F. J. *Chem. Phys.* **1985**, *83*, 735.
(50) Bader, R. F. W. *Atoms in Molecules, A Quantum Theory*; International Series of Monographs in Chemistry; Oxford University Press: Oxford, U.K., 1990; Vol. 22.
(51) Biegler−Künig, F.; Schünbohm, J.; Derdau, R.; Bayles, D.; Bader, R. F. W. *AIM 2000*, version 2.0; McMaster University: 2002.

(52) Kosov, D. S.; Popelier, P. L. A. *J. Phys. Chem. A* **2000**, *104*, 7339.
(53) (a) Angyan, J. G.; Loos, M.; Mayer, I. *J. Phys. Chem.* **1994**, *98*, 5244. (b) Angyan, J. G.; Jansen, G.; Loos, M. C. H.; Hess, B. A. *Chem. Phys. Lett.* **1994**, *219*, 267.
(54) Zhou, H. W.; Wong, N.-B.; Zhou, G.; Tian, A. M. *J. Phys. Chem. A* **2006**, *110*, 3845.
(55) (a) Yamaguchi, K.; Jensen, F.; Dorigo, A.; Houk, K. N. *Chem. Phys. Lett.* **1988**, *149*, 537. (b) Soda, T.; Kitagawa, Y.; Onishi, H.; Takano, Y.; Shigeta, Y.; Nagao, H.; Yoshioka, Y.; Yamaguchi, K. *Chem. Phys. Lett.* **2000**, *319*, 223.
(56) Sato, T. A.; Tsuneda, T. B.; Hirao, K. *J. Chem. Phys. A* **2005**, *123*, 1.
(57) Molina, J. M.; Dobado, J. A.; Daza, M. C.; Villaveces, J. L. *J. Mol. Struct.* (*THEOCHEM*) **2002**, *580*, 117.
(58) Cullen, J. *Chem. Phys.* **1996**, *202*, 217.
(59) Voorhis, T. V.; Head-Gordon, M. *J. Chem. Phys.* **2000**, *112*, 5633.
(60) Kong, J.; White, C. A.; Krylov, A. I.; Sherrill, D.; Adamson, R. D.; Furlani, T. R.; Lee, M. S.; Lee, A. M.; Gwaltney, S. R.; Adams, T. R.; Ochsenfeld, C.; Gilbert, A. T. B.; Kedziora, G. S.; Rassolov, V. A.; Maurice, D. R.; Nair, N.; Shao, Y. H.; Besley, N. A.; Maslen, P. E.; Dombroski, J. P.; Daschel, H.; Zhang, W. M.; Korambath, P. P.; Baker, J.; Byrd, E. F. C.; Voorhis, T. V.; Oumi, M.; Hirata, S.; Hsu, C. P.; Ishikawa, N.; Florian, J.; Warshel, A.; Johnson, B. G.; Gill, P. M. W.; Head-Gordon, M.; Pople, J. A. *J. Comput. Chem.* **2000**, *21*, 1532.
(61) Schmidt, M. W.; Baldridge, K. K.; Boatz, J. A.; Elbert, S. T.; Gordon, M. S.; Jensen, J. H.; Kosecki, S.; Matsunaga, N.; Nguyen, K. A.; Su, S. J.;Windus, T. L.; Dupuis, M.; Montgomery, J. A. J. *Comput. Chem.* **1993**, *14*, 1347.